

1 Stochastic analysis of the efficiency of coupled hydraulic-physical 2 barriers to contain solute plumes in highly heterogeneous aquifers

3 Daniele Pedretti^{1,*}, Marco Masetti², Giovanni Pietro. Beretta²

4 ¹Geological Survey of Finland (GTK), Espoo, Finland

5 ²Dipartimento di Scienze Della Terra “A. Desio”, Università degli Studi di Milano, Milan, Italy

6 *Corresponding author: daniele.pedretti@gtk.fi

7 Abstract:

8 The expected long-term efficiency of vertical cutoff walls coupled to pump-and-treat
9 technologies to contain solute plumes in highly heterogeneous aquifers was analyzed. A well-
10 characterized case study in Italy, with a hydrogeological database of 471 results from hydraulic
11 tests performed on the aquifer and the surrounding 2-km-long cement-bentonite (CB) walls, was
12 used to build a conceptual model and assess a representative remediation site adopting coupled
13 technologies. In the studied area, the aquifer hydraulic conductivity K_a [m/d] is log-normally
14 distributed with mean $E(Y_a) = 0.32$, variance $\sigma_{Y_a}^2 = 6.36$ ($Y_a = \ln K_a$) and spatial correlation
15 well described by an exponential isotropic variogram with integral scale less than 1/12 the
16 domain size. The hardened CB wall's hydraulic conductivity, K_w [m/d], displayed strong scaling
17 effects and a lognormal distribution with mean $E(Y_w) = -3.43$ and $\sigma_{Y_w}^2 = 0.53$ ($Y_w =$
18 $\log_{10} K_w$). No spatial correlation of K_w was detected. Using this information, conservative
19 transport was simulated across a CB wall in spatially correlated 1-D random Y_a fields within a
20 numerical Monte Carlo framework. Multiple scenarios representing different K_w values were
21 tested. A continuous solute source with known concentration and deterministic drains' discharge
22 rates were assumed. The efficiency of the confining system was measured by the probability of

23 exceedance of concentration over a threshold (C^*) at a control section 10 years after the initial
24 solute release. It was found that the stronger the aquifer heterogeneity, the higher the expected
25 efficiency of the confinement system and the lower the likelihood of aquifer pollution. This
26 behavior can be explained because, for the analyzed aquifer conditions, a lower K_a generates
27 more pronounced drawdown in the water table in the proximity of the drain and consequently a
28 higher advective flux towards the confined area, which counteracts diffusive fluxes across the
29 walls. Thus, a higher $\sigma_{Y_a}^2$ results in a larger amount of low K_a values in the proximity of the
30 drain, and a higher probability of not exceeding C^* .

31 *Keywords: cutoff walls, aquifer heterogeneity, solute transport, risk, uncertainty, pump-and-treat*

32

33 **1. Introduction**

34 The combination of hydraulic and physical barriers has been adopted for decades for the
35 remediation of solute polluted aquifers. A well-known approach is for instance the use of pump-
36 and-treat technologies combined with vertical cutoff walls (e.g. Bayer and Finkel, 2006; Beretta,
37 2015; Pedretti et al., 2013a). The accurate hydraulic design of combined pump-and-treat systems
38 (CP&Ts) requires a reliable parameterization of the hydrogeological properties of both the
39 physical barriers and the surrounding aquifer. These issues have been documented in multiple
40 analyses presented in the past (e.g. Bayer and Finkel, 2006; Beretta, 2015; Britton et al., 2005;
41 Kaleris and Ziogas, 2013; Khandelwal et al., 1997; Pedretti et al., 2011; Russell and Rabideau,
42 2000; Wu et al., 2016; Xanthakos, 1979).

43 The hydraulic conductivity of the aquifer (K_a) and the hydraulic conductivity of the vertical
44 cutoff walls (K_w) are two of the key parameters for the hydrogeological design of CP&Ts. These
45 parameters control the net balance between inward and outward advective and diffusive solute
46 fluxes across the walls. Outwards refers here to solute fluxes from the cutoff-wall- confined area
47 towards the clean aquifer. Inwards indicates the opposite flux direction. These concepts are well
48 explained for instance by Devlin and Parker (1996) and Neville and Andrews (2006). In short,
49 when the sum of outward fluxes exceeds the sum of inward fluxes, some solute particles are able
50 to escape the confined system, creating potential environmental, social and economic risks. For
51 instance, a concern is created when the concentrations exceed a predefined threshold established
52 by local regulations. On the other hand, if the total inward flux is equal or larger than the total
53 outward fluxes, no solute particles escape the confined system and no risks exist.

54 Because of the limited accessibility to the subsurface and the high cost of explorations, the
55 ubiquitous hydraulic heterogeneity of geological sites is never adequately characterized. This
56 complicates the reliability of predictions regarding the expected behavior of the aquifers and the
57 CP&T systems, when present. Lack of complete characterization of hydrogeological
58 heterogeneity generates an epistemic type of randomness and uncertainty in the decision-making
59 process, such as for risk assessment and aquifer remediation. In this context, stochastic-based
60 modeling analysis provides a suitable approach tool to support decision makers when making
61 predictions with a quantitative estimation of the expected model behavior and associated
62 uncertainty (e.g. Tartakovsky, 2007). Unfortunately, stochastic modeling has not been yet
63 routinely adopted by practitioners (e.g. Renard, 2007; Sanchez-Vila and Fernández-Garcia,
64 2016) and more efforts are required to researchers in order to illustrate the actual benefits of

65 stochastic modeling against traditional deterministic approaches to quantify flow and transport
66 under uncertain aquifer conditions.

67 The majority of documented stochastic analyses in hydrogeology have mainly targeted K_a as a
68 primary source of randomness and uncertainty (e.g. Dai et al., 2004; Kawas and Karakas, 1996;
69 Kitanidis, 1988; Sanchez-Vila et al., 1996). Yet, the presence of cutoff walls can add further
70 variability to the behavior of the aquifers (e.g. Elder et al. 2002, Hemsli and Shackelford 2006).

71 This occurs mainly since (1) the hydraulic characterization of vertical cutoff walls may be
72 complex and expensive as much as for (or more than) the characterization of aquifers, and (2) the
73 strong scaling effects of K_w measurements, especially when comparing laboratory-based and in-
74 situ estimations (Britton et al., 2005; Daniel, 1984; Joshi et al., 2009; Manassero, 1994). In the
75 case of cement-bentonite (CB) walls, the latter issue poses severe difficulties for the accurate
76 design of the physical confinement. The synthetic mixture placed in the ground to form the CB
77 walls after cement curing or hardening is designed in laboratory. The resulting hydraulic
78 conductivity of this perfectly mixed hardened liquid is firstly estimated under laboratory-
79 controlled conditions, which are generally not representative of field conditions. Indeed,
80 laboratory-based conductivities are expected to be of the order of $K_w=10^{-8}$ m/s (e.g. Turchan et
81 al., 1989) or lower. When released in a soil trench or similar excavation, undetected
82 hydrogeological heterogeneities in the surrounding aquifer or inhomogeneous mixing of
83 chemical solutions can result in undesired cracks and fissures following the CB wall's hardening.

84 In-situ K_w is therefore generally larger than laboratory-based K_w , by some orders or magnitude
85 (e.g. Britton et al., 2005; Daniel, 1984; Joshi et al., 2009; Manassero, 1994). Making *a priori*
86 estimations of the magnitude of this scale-dependent difference remains however challenging in
87 the practice.

88 The implication of the uncertainty related to the hydraulic properties of physical walls
89 (variability of K_a) in presence of heterogeneous aquifer conditions (variability of K_w) has not
90 been studied exhaustively. Britton et al. (2005) used a lognormal distribution of K_w to study
91 contaminant flux through a cutoff-wall with idealized initial and boundary conditions and
92 surrounded by a homogeneous aquifer. They showed that an increase in variability of the wall's
93 hydraulic conductivity determines an increase in solute flux across the walls, since a larger K_w
94 increase the flux escaping the wall compared to the flux evaluated using only the average
95 hydraulic conductivity of the walls. They concluded that estimates of contaminant flux may be
96 incorrect if the variability of K_w is not taken into account.

97 These issues motivate this paper, in which we developed a stochastic model based on numerical
98 Monte Carlo (MC) simulations of conservative transport to examine the implication of combined
99 aquifer and CB wall's variability on the effectiveness of a CP&T configuration to contain a
100 solute plume. Our goal is to provide answers to questions such as:

- 101 1. How much does the lack of complete knowledge of K_a and K_w affect the expected
102 efficiency of the CP&T system?
- 103 2. How uncertain is this estimation, for different degree of heterogeneity of the aquifer and
104 for different combination of CB walls?

105 To this end, we operated within a classic stochastic framework based on the solution of
106 ensembles of MC results from the solution of transport in randomly varying correlated fields
107 (realizations) of aquifer's hydraulic conductivity and according to different testing scenarios of
108 CB wall conductivity. In each realization, we simulated flow and transport using a conceptual
109 model and boundary conditions that resemble the CP&T and aquifer configuration observed
110 from a former Italian SIN site (acronym for Site of National Interest, comparable to a US

111 superfund site). We chose this site as a representative well-characterized working example to
112 apply the stochastic model. In particular, we had access to a hydrogeological database with 414
113 results from hydraulic conductivity tests performed on the local CB walls at different scales and
114 64 results from pumping tests performed at different locations (boreholes) of the surrounding
115 unconfined sedimentary aquifer. These unique results allowed for an exhaustive geostatistical
116 assessment of the variability of K_a and K_w and provided the basis to formulate a realistic
117 stochastic assessment. Our framework allows providing quantitative estimation of the expected
118 efficiency of the CP&T system and the associated uncertainty around the mean. Such an
119 efficiency is measured through the probability that solute concentrations exceed a predefined
120 concentration threshold at a control section outside the polluted area over time. We are then able
121 to provide an answer to our initial questions, (1) by directly relating the random variability of K_a
122 and K_w to the expected likelihood of pollution of the clean aquifer surrounding the confined site,
123 and (2) by evaluating the uncertainty affecting the mean behavior of the aquifer, quantitatively
124 associated with the variability of hydrogeological properties of the site. To ensure that results are
125 exportable to other field conditions, our analysis covers K_w values ranging from the entire
126 spectrum of typical hydraulic conductivities reported in operations with CB walls. In particular,
127 we studied walls with progressive increase of walls' hydraulic conductivities from $K_w = 10^{-9}$
128 m/s to values approaching the hydraulic conductivities of the aquifer ($K_w \rightarrow K_a$).

129 The paper is structured as follows. Section 2 provides an overview of the site, including some
130 historical information regarding the source of pollution and the chronology of the plume
131 confining activities. Section 3 introduces the hydrogeological database. We describe the type of
132 hydraulic tests that were performed on the aquifer and the CB walls, the solution adopted to
133 estimate K_a and K_w at the different location, and the results of the geostatistical analysis. Section

134 4 presents the methodology and results from the stochastic analysis, including the model
135 implementation, the adopted governing partial differential equations and related mathematical
136 solutions. Here, the key results from the analysis are presented and discussed. Limitations of the
137 study and future developments are also addressed in Section 4. The manuscript ends with the
138 main conclusions drawn from this work.

139 **2. Case study overview**

140 The analyzed system (Figure 1) is located underneath a decommissioned chemical facility nearby
141 Cengio (Italy). Since 1882, a large portion of this land (approximately 122 ha) was used to
142 dispose chemical wastes and refuse materials by dumping and burying them in the ground
143 without hydrogeological control (Domenico et al., 1992). The prevalent soil contaminants were
144 metals (As, Cr, Hg, Ni, Cu, Pb, Zn), hexachlorobenzene, aromatic halogenated compounds,
145 phenols, aromatic amines, nitrobenzenes, dioxins, furan, PAH and PCB. This resulted in a
146 multicomponent solute plume which has persistently damaged the local ecosystem and severely
147 affected the watersheds downstream the facility. The site has received a great attention at the end
148 of the 1900s due to the high concentration of heavy metals and aromatic hydrocarbons observed
149 in the neighboring Bormida di Millesimo river (Baldi et al., 2007). Detected contaminants were
150 Al, As, Fe, Mn, Pb and naphthalenesulfonic compounds. Water discharges over a century are
151 believed to have affected an area of over 22000 ha in Liguria and Piemonte regions. In the late
152 1990s, multiple remediation activities were started, most of which were funded by the Italian
153 Government. They included the installation of multiple CB walls, aiming to confine the pollution
154 within the source and prevent the direct contact of the solute plume with the river (De Paoli and
155 Marcellino, 1992; Maione, 1995) and the construction of landfills to store chemical wastes and

156 part of the contaminated soils. Since then, several advanced remediation activities have been
157 documented related to this site (e.g. D’Annibale et al., 2005; Domenico et al., 1992; Falasco et
158 al., 2009). Nowadays, the contamination is controlled and the Bormida di Millesimo river water
159 has been recently classified as of good quality (Durante and Grasso, 2010).

160 [FIGURE 1: HERE]

161 The former chemical site lies on an unconfined heterogeneous 1-to-20-m-thick aquifer composed
162 of a mixture of natural soil (alluvium), chemical waste, building debris and other byproducts.
163 Below the aquifer, the marl bedrock creates an impervious aquiclude, with thickness over 100 m
164 in the local area. A series of Lugeon tests indicate the good quality of the bedrock all over the
165 area, giving maximum hydraulic conductivity values of about 10^{-9} m/s. During the remediation
166 activities, only the main point sources of contamination had been physically removed from the
167 aquifer by dig and dump operations, but almost all the rest of area remains affected by the
168 presence of contamination. Both anthropic and natural alluvial soils act as a diffuse source of
169 multicomponent solute contamination.

170 The aquifer is recharged by direct rainfall infiltration, hill slope runoff and lateral underground
171 influx. No significant groundwater flow occurs along the uphill contact between unconsolidated
172 deposit and the marl formation, due to the extremely limited groundwater circulation in the marl.
173 The distance from the farthest recharge location to the discharging drain is about 1000m,
174 although the main sparsely distributed sources of contamination can be located at closer
175 distances from the drains in the center of the river bend (in correspondence of the label “former
176 chemical facilities” in Figure 1a). The aquifer used to discharge directly to the Bormida di
177 Millesimo River, although today multiple vertical cutoff walls and drains create an impervious
178 confinement to isolate the source of pollution within the river bend. The hydraulic pumping

179 system is designed to pump out all the groundwater flux and treat it *ex-situ*, before being
180 redirected to the river.

181 The results presented in this work refer to the first 2-km-long CB wall created in the early 2000s
182 to isolate the contaminated soil (Figure 1a). The wall was nailed into the impervious marl
183 bedrock and combined with an initial draining system, which collected the polluted water and
184 created an inward head gradient to contrast outward diffusive solute fluxes, as conceptually
185 shown in Figure 1b. A large characterization activity was performed to measure the variability of
186 K_a and K_w at different points of the aquifer and locations (zones) along the wall at different CB
187 hardening times. Part of the results was collected and available for this study. No raw data
188 existed, however, such that we could not test the actual reliability and accuracy of the pre-
189 interpreted results. We note that this issue does not directly affect our conclusions. Indeed, the
190 case study and this database were analyzed with the primary purpose of providing representative
191 and realistic preliminary information for our stochastic analysis and obtain general conclusions
192 regarding the ability of CP&T sites to contain solutes under hydrogeological uncertainty.

193 **3. Analysis of the hydrogeological database**

194 **3.1. Aquifer hydraulic conductivity**

195 The database contained 64 measurements of K_a , which represent the aquifer hydraulic
196 conductivity estimated from an equivalent number of boreholes sparsely located in the site after a
197 series of conventional pumping tests. The tests were pre-interpreted and no raw data were
198 available to ensure the actual correctness of the interpretation, which is assumed as valid. The
199 location of the boreholes is schematically shown in Figure 2a. This figure also highlights the

200 mean direction of groundwater flux in the aquifer, which is conditioned by the presence of the
201 continuous drain in the proximity of the CB walls.

202 We used these results to perform a geostatistical analysis to estimate the spatial and global
203 variability of K_a in the aquifer. Figure 2b shows the experimental variogram of $Y_a = \ln(K_a)$ at
204 different lags, overlapped by the exponential model used to parameterize the spatial variability of
205 Y_a . The exponential model for unit variance has form (e.g. Gooverts, 1997, p.90)

$$206 \quad \gamma(r) = 1 - \exp\left(-\frac{3r}{d}\right) \quad (1)$$

207 where r is the distance between two points [m] and d is the range [m]. The exponential
208 variogram (1) has a characteristic integral scale I [m], defined as $I = d/3$. Figure 2c and Figure
209 2d illustrate the empirical histogram and cumulative density of Y_a , respectively.

210 We found that the aquifer is characterized by a univariate log-normally distributed hydraulic
211 conductivity distribution with mean $E(Y_a) = 0.32$ and variance $\sigma_{Y_a}^2 = 6.36$. After testing
212 isotropic and anisotropic variograms, an isotropic exponential variogram with range $d \approx 150$ m
213 ($I \approx 50$ m) was able to satisfactory describe the spatial variability of Y_a . These results have direct
214 implications for the selection of stochastic modeling framework to evaluate the implication of
215 aquifer and wall's variable hydraulic properties. The high variance of $\ln(K)$ suggests a very
216 strong aquifer hydraulic heterogeneity. Using a conservative approach and referring to the
217 geological trace on Figure 1a, let us consider a solute source located at A', which is
218 approximately the farthest point of the river bend at A (with $L \approx 600$ m) and use $I=50$ m. Under
219 these circumstances, a plume forming from the solute sources would only travel $L/I \approx 12$
220 integral scales before entering the river, which may be insufficient to ensure ergodic solute
221 transport within the studied domain. Indeed, under such high aquifer variances and uniform flow

222 conditions, solute particles should sample a much larger amount of heterogeneity (i.e. several l)
223 to become ergodic (e.g. Jankovic et al. 2006). When considering source locations closer to the
224 drains solute particles would travel for even fewer integral scales, magnifying the effects of non-
225 ergodicity. The presence of drains renders it even more difficult to define transport ergodicity,
226 for instance because flow is by definition not stationary under non-uniform conditions (e.g.
227 Matheron, 1967).

228 [FIGURE 2: HERE]

229 **3.2.CB walls hydraulic conductivity**

230 For the characterization of the CB wall, 407 K_w measurements collected at four unevenly
231 distributed zones of the CB wall (A, B, C, D in Figure 2a) were available from the historic
232 database. Zone D was the most characterized, while zone A was the least characterized.
233 Laboratory tests and three in-situ methods (CPTU, Geon-BAT piezometers and slug tests) were
234 performed using standard approaches and analytical method for the interpretation of the
235 hydraulic tests. The complete list of values by location or zone in the site, the type of
236 measurement and known analytical methods for their interpretation are reported in the
237 Supplementary Material.

238 Laboratory tests were performed at different hardening (i.e., curing) times from samples
239 collected on site and assessed using small-scale permeameters. Due to their relative simplicity
240 and low execution cost, laboratory tests represented the majority of the experimental database
241 (about 200 samples). The laboratory testing methodology followed standard procedures (ASTM
242 D5084-03).

243 In-situ tests were also performed at different curing times. Slug tests were performed on
244 micropiezometers, and K_w was estimated from the interpretation of hydraulic tests using the
245 method by Bouwer and Rice (1976). This type of tests is widely adopted for the analysis of in-
246 situ K_w , (e.g., Britton et al., 2002; Choi and Daniel, 2006; Choi et al., 2014; Lim et al., 2014;
247 Nguyen et al., 2010). CPTU tests were performed following the methodology by Manassero
248 (1994). The piezocone probe is characterized by a water-pressure transducer activated by a
249 grease fluid that fills a slot located just behind the cone shoulder. In the CPTU method, K_w is
250 estimated from the consolidation coefficient of CPTU dissipations through simple analytical
251 expressions. No direct information regarding the execution of the CPTU in the site (e.g. point
252 resistance and sleeve friction) was available for this study. The CPTU is able to provide a profile
253 of K_w along the vertical direction of piezocone penetration. However, for this study only
254 averaged K_w over a vertical section of the walls were available for different points of the barrier.
255 BAT piezometers (Torstensson, 1984) with pressure sensors were adopted at approximately 110
256 curing days. This technology is also based on an in-situ pore-pressure dissipation approach, as
257 the CPTU. In this case, a porous cell is introduced into the ground and isolated through a rubber
258 membrane. A vacuum sampler and a pressure transducer (connected to a data logger on the
259 surface) are introduced into the porous cell, and measure the relative change in pressure with the
260 aquifer. Similar to the CPTU, K_w is estimated from a set of precalibrated empirical relationships.
261 To the best of our knowledge, the Geon-BAT method has not been presented elsewhere for the
262 characterization of K_w .

263 Figure 3 illustrates the comparison of estimated K_w from laboratory and combined in-situ tests,
264 which emphasizes the impact of support scale on the measurements, at different curing times
265 (t_c). The dotted lines represent a best-fit regression curves obtained from a power-law model of

266 form $K_w \propto t_c^{-m}$. A first visual inspection confirms the existence of strong scaling effects in the
267 estimated hydraulic conductivity of the CB wall. K_w was found to be smaller for laboratory-scale
268 measurements than for in-situ measurement, consistent with previous investigations on vertical
269 cutoff walls (e.g. Britton et al., 2005; Joshi et al., 2009). Our analysis also suggests that the
270 characteristic hardening factor (m) is larger for in-situ measurements than for laboratory
271 samples. This may be related to the different behavior of CB mixture in the field compared to
272 laboratory conditions, and could be a possible reason of the resulting scaling effects in the
273 estimated conductivities (in addition to the other mechanisms previously described).

274 [FIGURE 3: HERE]

275 Figure 4a reports four boxplots summarizing the statistical distribution of in-situ K_w calculated
276 for an equivalent curing time $t_c=280$ days. This equivalent value is obtained by extrapolating
277 each in-situ measurement using the fitted power-law regression function, and useful to obtain a
278 larger dataset for statistical inference of the clustered data. These clusters are obtained by
279 subdividing the dataset into the four major zones (A,B,C,D) where the tests were performed, in
280 an attempt to obtain an indication of spatial structure or correlation in the distribution of K_w . Let
281 us now observe the boxplots, reminding that the width of each box is proportional to the number
282 of samples (n_s) used for the calculation of the empirical distributions. It can be observed that,
283 while n_s is smaller for zone A than for zone D, the median values are quite similar among all
284 locations, and 1st-to-3rd interquartile distance is also comparable between the four zones and
285 ranging in an interval comprised between 5×10^{-2} m/d and 5×10^{-3} m/d (i.e. about one order
286 of variability of K_w). In zone D, the extremes of the distribution seem to display a larger
287 variability than in zone A.

288 [FIGURE 4: HERE]

289 Figure 4b reproduces the statistical distribution of the combined K_w measurements from the four
290 zones. We found that the K_w of the entire CB wall is nicely described by a univariate log-normal
291 distribution with the mean $E(Y_w) = -3.43$, where $Y_w = \log_{10}(K_w)$. The resulting variance
292 $\sigma_{Y_w}^2 = 0.53$ is however much lower than that of the aquifer ($\sigma_{Y_w}^2 = 6.5$). The relative
293 homogeneity of the CB wall does not surprise, since all points of the cement-bentonite wall are
294 made up of the same chemical mixture, and the presence of defects associated to localized
295 cracks, fracture or in-situ inhomogeneity of the CB mixture can be considered as minor along the
296 wall from a hydraulic perspective. This also implies that, although we lack of sufficient
297 information for the spatial analysis of K_w , poor or no correlation of K_w is expected in space
298 along the wall. Indeed, CB walls are artificial structures created without a specific spatial-
299 dependent process, such as alluvial and glacial deposition or tectonic and post-tectonic
300 deformation as in the case of sedimentary or fractured formations, respectively.

301 **4. Stochastic analysis**

302 The experimental geostatistics obtained from the analysis of the historic database and the aquifer
303 configuration of the ACNA site provided a representative real-life example to develop the
304 stochastic modeling analysis targeting the efficiency of the CP&T system in heterogeneous
305 systems. The analysis is based on the solution of an ensemble of random synthetic realizations
306 within a Monte Carlo (MC) framework. The likely lack of transport ergodicity conditions implies
307 the use of MC-based numerical simulations under bounded flow domains (e.g. Pedretti et al.,
308 2014) to adequately evaluate the stochastic problem analyzed in this work. These aspects may
309 impede for instance the direct applications of more computationally efficient stochastic methods

310 such as effective analytical solutions (e.g. Dagan, 1989) which are formally valid for specific
311 conditions not applicable to our case study, such as unbounded domains and weak heterogeneity
312 ($\sigma_{Y_a}^2 \leq 1$).

313 **4.1.Model framework and setup**

314 We conceptualized the flow and transport model as graphically depicted in Figure 5. Because of
315 the presence of continuous drain pumping in the analyzed aquifer, the mean direction on the
316 groundwater flux was perpendicular to the CB wall at all points along the wall. In addition, no
317 well-defined point source of pollution existed in the domain, but rather the entire confined
318 aquifer played the role as a macroscopic sparsely distributed source, which threatened the
319 pollution of the nearby Bormida di Millesimo river.

320 [FIGURE 5: HERE]

321 Based on this knowledge, we idealized a one-dimensional (1D) unconfined heterogeneous
322 aquifer, which was discretized and solved using the finite-difference code MODFLOW-96
323 (Harbaugh and McDonald, 1996). Each cell had a top elevation of 15 m and a bottom elevation
324 of 0 m. The total length of the domain was 1000 m. The domain was oriented along the mean
325 groundwater flow direction and parallel to the x coordinate of a Cartesian reference grid. The
326 system was discretized with a telescopic refinement towards the central region of the domain. In
327 the middle of the domain (i.e. nearby the source of pollution, the drain and the CB wall) the cell
328 size was 0.1 m and increased with a logarithmic-based increment towards the boundaries, with a
329 maximum cell size of 1 m. The flow boundary conditions were imposed to create, under
330 unpumped conditions, a natural gradient equal to 0.001. The model was recharged by prescribed-
331 head boundary conditions at one side of the domain and discharges at the other side, as in Figure

332 5. To create pumped conditions, we imposed a drain condition in one cell of the domain, with a
333 constant deterministic pumping rate Q_w . A set of cells with different hydraulic conductivity than
334 the remaining cells of the domain formed the CB wall, with thickness 1m and adjacent to the
335 drain.

336 We generated two sets of $n_{MC}=1000$ random fields of Y_a . Both sets were generated using a
337 variogram-based Sequential Gaussian Simulation (SGS) algorithm coded within SGEMS (Remy
338 et al., 2009). The first set was generated using an exponential variogram (Eq. 1) similar to the
339 one obtained from the hydrogeological database, with range $d=150\text{m}$ and sill (i.e. variance)
340 $\sigma_{Y_a}^2 = 6.5$. The second set was developed to study an aquifer with a milder heterogeneity; we
341 imposed the same variogram structure as for the first set of simulations, but with sill $\sigma_{Y_a}^2 = 1$.
342 The Y_a values from the two sets of SGS simulations were transformed into K_a and used as
343 hydraulic conductivity parameters in MODFLOW-96.

344 Because of 1-D nature of our models and the lack of experimental information regarding the
345 vertical variability of K_w values, we could not adopt the approach of Britton et al. (2005).
346 Instead, we simulated three scenarios, each of which embedding a different homogeneous CB
347 wall hydraulic conductivity. Each homogeneous K_w value can be seen as an effective (or
348 upscaled) CB wall's hydraulic conductivity which lumps together the variability of K_w due to
349 local cracks and fissures that can be found along the vertical direction of the walls.

350 For each realization in each set of SGS simulations and for each K_w scenario, we obtained an
351 ensemble of flow fields from MODFLOW-96 which were used as input for an analogous number
352 of 1-D transport simulations based on the advection-dispersion-equation (ADE) model. We
353 simulated transport of an idealized conservative species using the code MT99 (Zheng and Wang,

1999), which is efficiently coupled to MODFLOW-96. A similar approach was already successfully used for the analysis of transport across low-permeable barriers in homogeneous settings (e.g. Devlin and Parker, 1996; Hudak, 2004; Neville and Andrews, 2006). The ADE is defined upon the groundwater flux q [m/d] calculated using MODFLOW-96, an effective kinematic porosity ϕ [-] and a hydromechanical effective scale-invariant local dispersion term $D = D^* + \alpha_L |v|$, where D^* is the effective diffusion coefficient [m²/d], α_L is the longitudinal dispersion [m] and $v = q/\phi$. The solution of the ADE, obtained using a TVD algorithm, is a concentration C [mg/L] of the solute species in space x [m] and time t [d]. We arbitrarily assumed homogeneous $D^* = 10^{-5}$ m²/d, $\alpha_L = 0.1$ m and $\phi = 0.1$, such that the entire variability of the solution is uniquely associated to the variability of K_a and K_w (our primary targets). Transport was calculated for each realization in both sets of SGS realizations and each of the three K_w scenarios. In all realizations, we assumed $C(x, t_0) = 0$, i.e. a pristine aquifer at initial time, except at one cell in which we imposed a constant concentration (C_0) throughout the entire simulation time. This cell simulates a continuous source of contaminant spilling from the upgradient side of drain (Figure 5) and occurring immediately at t_0 .

4.2. Analysis and discussion

We calculated the efficiency of the CP&T from the probability that C exceeds an arbitrary predefined threshold C^* at $t=10$ years at a specific model cell (Figure 5), acting as an observation piezometer (passive borehole), at which we tracked the evolution of concentration as a resident breakthrough curve (BTC). For illustrative purposes, we selected an arbitrary realistic dimensionless maximum concentration threshold $C_{max} = C^*/C_0 = 10^{-4}$, or $\log_{10}(C_{max}) = -4$. This threshold represents for instance a maximum concentration threshold of 0.1 mg/L

376 occurring for a spill with concentration of 100 mg/L. The targeted piezometer is located
377 downgradient of the solute source in order to track the concentration at a piezometer located
378 outside the confined area within the pristine part of the aquifer potentially threatened by the
379 solute plume. We chose to monitor the first cell adjacent to the vertical walls in order to
380 minimize the effects of concentrations dilution in other cells downgradient of the source.

381 We first recall the expected theoretical effect of the drains and the barrier on the system, and
382 their consequences on solute transport. In principle, the drain should lower the water table within
383 the unconfined aquifer, as conceptually shown in Figure 1b. If it does, the lowered water table
384 creates an artificial hydraulic head gradient between the two sides of the barrier. This gradient
385 should create an inward advective flux that contrasts the outwards diffusive flux. As such, the
386 efficiency of the CP&T system depends directly on the amount of inward advective flux versus
387 the outwards diffusive flux, which in turn depend on the hydraulic conductivities of aquifer
388 (which in our work are randomly varied in each simulation) and CB walls (which are varied by
389 scenarios).

390 We now evaluate how likely this theoretical behavior applies under hydrogeological randomness.
391 All the results from this analysis are summarized in Figure 6. Each panel reports the statistical
392 distribution of the ensemble of concentrations measured at the targeted piezometer at 10 years
393 from the initial spill and obtained from each specific set of simulation and K_w scenario. The
394 results are presented in three forms: the histogram of concentrations (blue bars), the cumulative
395 density function of the concentrations (red curve) and the ensemble-averaged concentration
396 (green dotted line). The concentrations are expressed as $\log_{10} (C/C_0)$, to be directly compared to
397 $\log_{10} C_{max}$. The ensemble mean expresses the expected behavior of each set of simulations and
398 scenario, and in turn the expected efficiency of the tested CP&T configuration. The top panels

399 show the results from the less heterogeneous set of SGS simulations ($\sigma_{Y_a}^2 = 1$), while the bottom
400 row shows the results for the high heterogeneous set of simulations ($\sigma_{Y_a}^2 = 6.5$). Each column
401 represents a different K_w value, which increases from left to right.

402 [FIGURE 6: HERE]

403 We first analyzed the set of simulations with lower heterogeneity (top rows of Figure 6). We
404 note from the green line that the ensemble-averaged concentration increases as K_w decreases.
405 This occurs since a higher mean hydraulic conductivity of the CB walls ensures a higher mean
406 inward advective flux that more efficiently contrasts the outwards diffusion. More specifically,
407 we found that for $K_w = 10^{-3}$ m/d, the normalized concentration is of the order of $\log_{10} (C/C_0) =$
408 -42 . This extremely low value has to be assumed as virtually zero, since from a practical
409 perspective such concentration would likely fall much below to the detection limit of typical
410 analytical approaches (considering C as expressed in mg/L). In addition, numerical stability may
411 affect the actual reliability of this number. For $K_w = 10^{-4}$ m/d, the expected concentrations is
412 slightly smaller than $\log_{10} (C/C_0) = -4$, suggesting that this CP&T configuration is in the limit of
413 providing an effective approach for the confinement and remediation of the contamination
414 plume, when compared to the selected maximum concentration threshold. For $K_w = 10^{-5}$ m/d,
415 the mean concentration exceeded C^* by several orders of magnitude and the system is clearly not
416 effective for the purpose of its application.

417 The analysis of the histograms and the corresponding CDFs reveals that the variability of the
418 concentrations around the mean value (which is directly associated to the variability of K_a fields
419 and directly measurable by $\sigma_{Y_a}^2$) affects the reliability of the ensemble mean as an informative
420 indicator about the actual efficiency of the CP&T. For $K_w = 10^{-3}$ m/d, the concentrations were

421 observed to fluctuate over 5 orders of magnitude around the mean. None of the realizations
422 detected a concentration above C^* , suggesting that the likelihood of pollution is negligible for
423 this scenario, even from a very conservative perspective. For the scenario with $K_w = 10^{-5}$ m/d,
424 the likelihood of aquifer pollution is maximum, since C^* is always exceeded by all the
425 realizations. In the intermediate case with $K_w = 10^{-4}$ m/d, however we observed that the
426 distribution is quite symmetric around the mean. In this specific scenario, it occurred by chance
427 that the mean also corresponds to the maximum concentration threshold. Because of that, and
428 observing the CDF, it is easy to infer that C^* is exceeded by about 50% of the total realizations.
429 In other words, the probability that one individual aquifer out of the polluted site will be polluted
430 after 10 years is 50%. When generalized to other field studies with boundary conditions similar
431 to the one analyzed in this work, the result can be also read as if one out of two aquifers
432 embedding this CP&T configuration and having $\sigma_{Y_a}^2 = 1$ will be polluted after 10 years.

433 The set of simulations with higher heterogeneity (bottom row of Figure 6) provides additional
434 important insights from this analysis. In this set of SGS simulations, the scenario with $K_w =$
435 10^{-3} m/d still ensures a great solution to contrast the downstream solute migration. Note
436 however that despite the normalized concentrations being very low, the mean has increased by
437 some 10 orders of magnitude compared to the same K_w in the set of SGS simulations with lower
438 variance. Moreover, although numerical stability may still play a role for such very low numbers,
439 the range of concentrations around the mean is now observed being >20 orders of magnitude
440 larger than for the simulations with lower $\sigma_{Y_a}^2$. For the case with $K_w = 10^{-5}$ m/d, the expected
441 concentration remains remarkably higher than the threshold C^* . However, in this case the
442 expected concentration is lower than in same K_w scenario for the low heterogeneity settings,
443 suggesting that an increase in heterogeneity generates (on average) a better general efficiency of

444 the CP&T under the same CB wall conditions. It is noted that the range of variability of the
445 concentrations has significantly increased even for this scenario, an effect once again associated
446 with the increase in $\sigma_{Y_a}^2$.

447 It is critical to observe and analyze the behavior of the CP&T embedding $K_w = 10^{-4}$ m/d of the
448 set of simulations with higher heterogeneity. Here, we found that the average concentrations
449 have dropped to $\log_{10}(C/C_0) \approx -6$, which is two orders of magnitude lower than the same result
450 for lower heterogeneity, and also than the threshold C^* . This issue confirms that (on average) the
451 more heterogeneous system is expected to better contain the solute plume than the more
452 homogeneous system. In addition, the analysis of the histograms and CDFs reveals that for
453 $\sigma_{Y_a}^2 = 6.5$ there is a significant fluctuation of measured concentrations around the mean
454 (spanning over about 8 orders of magnitude). However, about 20% of the simulations exceeded
455 the critical threshold C^* , or in other terms that the probability of aquifer pollution is one out of
456 five aquifers. This means that for $\sigma_{Y_a}^2 = 6.5$ the estimated likelihood of aquifer pollution is less
457 than one half the likelihood of aquifer pollution estimated for $\sigma_{Y_a}^2 = 1$.

458 Apart of the scenario with $K_w = 10^{-3}$ m/d, which may be affected by numerical instability, the
459 results suggest that simulations based on $\sigma_{Y_a}^2 = 6.5$ show a higher mean efficiency than those
460 based on $\sigma_{Y_a}^2 = 1$. To explain why this is occurring, we recall the behavior of these systems
461 under homogeneous conditions and considering the selected type of boundary conditions and
462 aquifer parameterization. For mass balance and under the same Q_w , an aquifer with a lower K_a
463 experiences more pronounced drawdown in the water table than an aquifer with a higher K_a to
464 maintain the same flux (e.g. Devlin and Parker, 1996; Neville and Andrews, 2006). This creates
465 a more pronounced drawdown head gradient across the barrier and a higher advective flux. For

466 the same K_w , a lower K_a value reduces diffusive fluxes more efficiently across the walls than for
467 a higher K_a value. Unlike homogeneous systems, however, our simulations embed a range of
468 correlated K_a values drawn from lognormal distributions. By definition, this distribution, which
469 is typically observed in nature (e.g. Freeze, 1975) and not merely valid for the site-specific
470 conditions analyzed here, generates more K_a values below the $E(Y_a)$ than values above the
471 $E(Y_a)$. Thus, a heterogeneous correlated field with mean $E(Y_a) = 0$ and $\sigma_{Y_a}^2 = 6.5$ has a much
472 larger probability of generating low K_a value than a heterogeneous field with mean $E(Y_a) = 0$ and
473 $\sigma_{Y_a}^2 = 1$, and thus a higher probability of more pronounced drawdown induced by the drain. To
474 quantitatively support this interpretation, Figure 7 reports the statistical distribution of maximum
475 drawdown observed nearby the drains for the six scenarios analyzed in this work. It is noted that
476 the scenarios embedding $\sigma_{Y_a}^2 = 6.5$ (right-hand boxplots) generate more drawdown than those
477 embedding $\sigma_{Y_a}^2 = 1$ (left-hand boxplots). It is important to note that this is true independently
478 from the selection of K_w .

479 [Figure 7 : HERE]

480 **4.3. Limitation and future developments**

481 Our analysis aims to target primarily the spatial variability of K_a and K_w as the key source of
482 uncertainty. Some important aspects that can potentially control the long-term estimation of the
483 effectiveness of the CP&T system have been left outside this study. They include, for instance,
484 the temporal change in CB walls conditions associated with the durability of the cement-
485 bentonite mixtures (e.g. Inyang and Tomassoni, 1992), such as the chemical attack of aquifer
486 contaminants with the soil-bentonite mixtures (e.g., Carreto et al., 2015; Malusis and McKeehan,

487 2013). These aspects require a non-trivial modeling approach (e.g. nonlinear time-dependent K_w
488 parameterization and reactive transport modeling analysis). Another aspect to be considered is
489 that the strong heterogeneity of the system could result in preferential flow paths, which may
490 require a different type of modeling analyses to be properly understood. Indeed, preferential flow
491 paths in bounded systems could be either reproduced via multidimensional flow modeling, such
492 as 3-D simulations (e.g. Pedretti et al., 2013b) or via effective 1-D models in which preferential
493 flow is associated with connected, highly mobile paths and embedded into a less mobile matrix
494 (e.g. Molinari et al., 2015). The implication of these aspects for the effectiveness of coupled
495 systems will be investigated in future developments.

496 **Summary and conclusion**

497 The combination of pump-and-treat technologies and vertical cutoff walls is a common solution
498 for the remediation of solute plumes in polluted aquifers. The design of these systems requires a
499 correct parameterization of the hydrogeological properties of both the physical barriers and the
500 surrounding aquifer. The presence of heterogeneity complicates the assessment of these
501 parameters, generating uncertainty in the reliability of model predictions and requiring a
502 stochastic modeling approach to be properly evaluated.

503 We adopted a stochastic modeling approach to study the expected long-term efficiency of the
504 remediation system to contain solute plumes in highly heterogeneous aquifers, using a
505 hydrogeological database from a well-characterized case study in Italy. The hydrogeological
506 setup of this site, commonly found in application of plume confinement and remediation in
507 alluvial aquifers is used to draw the working conceptual site model. The database contained 471
508 results from pre-elaborated in-situ and laboratory tests performed to characterize the hydraulic

509 conductivity of the aquifer and the 2-km-long cement-bentonite (CB) walls. Based on a
510 geostatistical analysis of this database and site, we developed a one-dimensional (1D) stochastic-
511 based modeling framework evaluating different scenarios of randomly variable aquifer
512 heterogeneity (K_a) and effective hydraulic conductivity of the barrier (K_w).

513 From the analysis of the results presented in the paper, we conclude that (1) the presence of
514 aquifer heterogeneities, (2) the difficulties to select an adequate K_w and (3) the uncertain scaling-
515 up of laboratory-estimated K_w into field-scale counterparts render the management of polluted
516 aquifer difficulties, with potential risk to exceed predefined thresholds of contaminant
517 concentrations at targeted vulnerable zone. More specifically,

- 518 • heterogeneity was seen to play a major role for the long-term assessment of the
519 effectiveness of the confinement system;
- 520 • for a given effective K_w , the increase of aquifer heterogeneities (here condensed into a
521 single indicator $\sigma_{Y_a}^2$, i.e. the variance of the univariate $\ln(K_a)$ distribution) determines, on
522 average, an increase in efficiency of the confinement system for the analyzed 1D system;
- 523 • the increase of aquifer heterogeneities adds more uncertainty regarding the optimal
524 hydraulic design of the system, adding uncertainty in the optimal strategies for the
525 effective management of solute plumes over long time scales.
- 526 • a very low value of K_w may not be necessarily beneficial for an effective aquifer
527 remediation.

528 The last conclusion is drawn considering that a low K_w requires higher drawdowns in the
529 polluted aquifer to maintain sufficiently steep hydraulic gradients across the barrier to generate
530 advective groundwater flux counterbalancing outwards solute diffusive flux (higher drawdowns

531 may not be easily overcome by increasing the pumping rates, for instance due to limited costs or
532 aquifer transmissivity).

533 In light of the well-known misconceptions regarding stochastic analysis, which limit its routine
534 use among practitioners (e.g. Renard, 2007; Sanchez-Vila and Fernández-García, 2016), our
535 study showed that it is indeed possible to bridge the gap between stochastic theory and
536 application by means of efficient calculation tools and using traditional measurements from
537 physically and hydraulic barriers. It is acknowledged that our conclusions are valid, provided the
538 conditions of applicability of the selected model analysis are fulfilled. For instance, ADE-based
539 1D models may not be able to effectively describe preferential flow and channeled transport,
540 which may occur in heterogeneous media. Moreover, conservative transport cannot reproduce a
541 possible time-dependent change in the walls' hydraulic properties due to the interaction between
542 solute plume and cement-bentonite matrix. The extension of our modeling analysis to
543 multidimensional and reactive systems is left open for future developments.

544 **Acknowledgments**

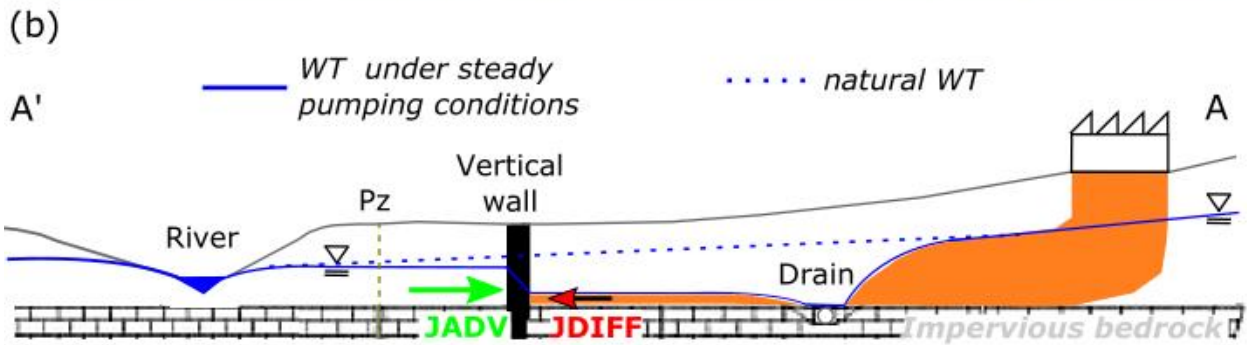
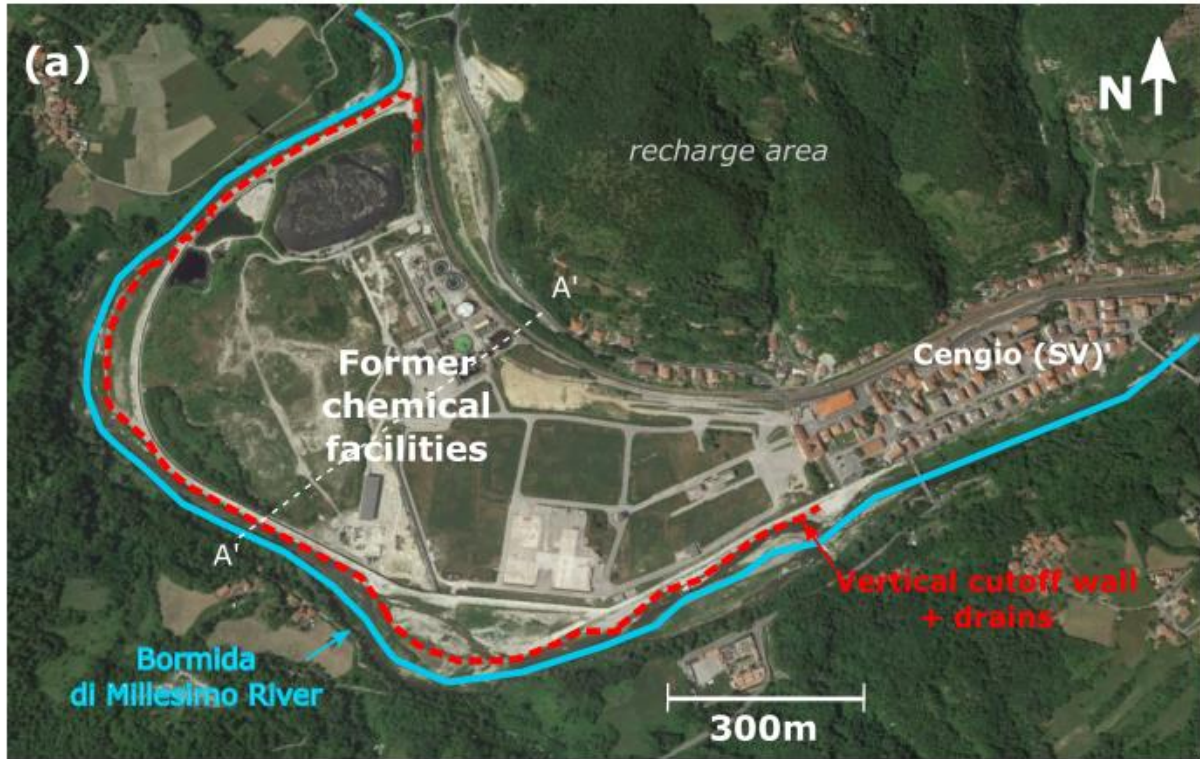
545 The authors acknowledge Dr. Stefano Veggi for his initial contribution to this research providing the
546 hydrogeological database. The authors acknowledge the Editors and the two anonymous Reviewers who
547 provided useful suggestions to improve our manuscript.

548

549

550 **Figures and captions**

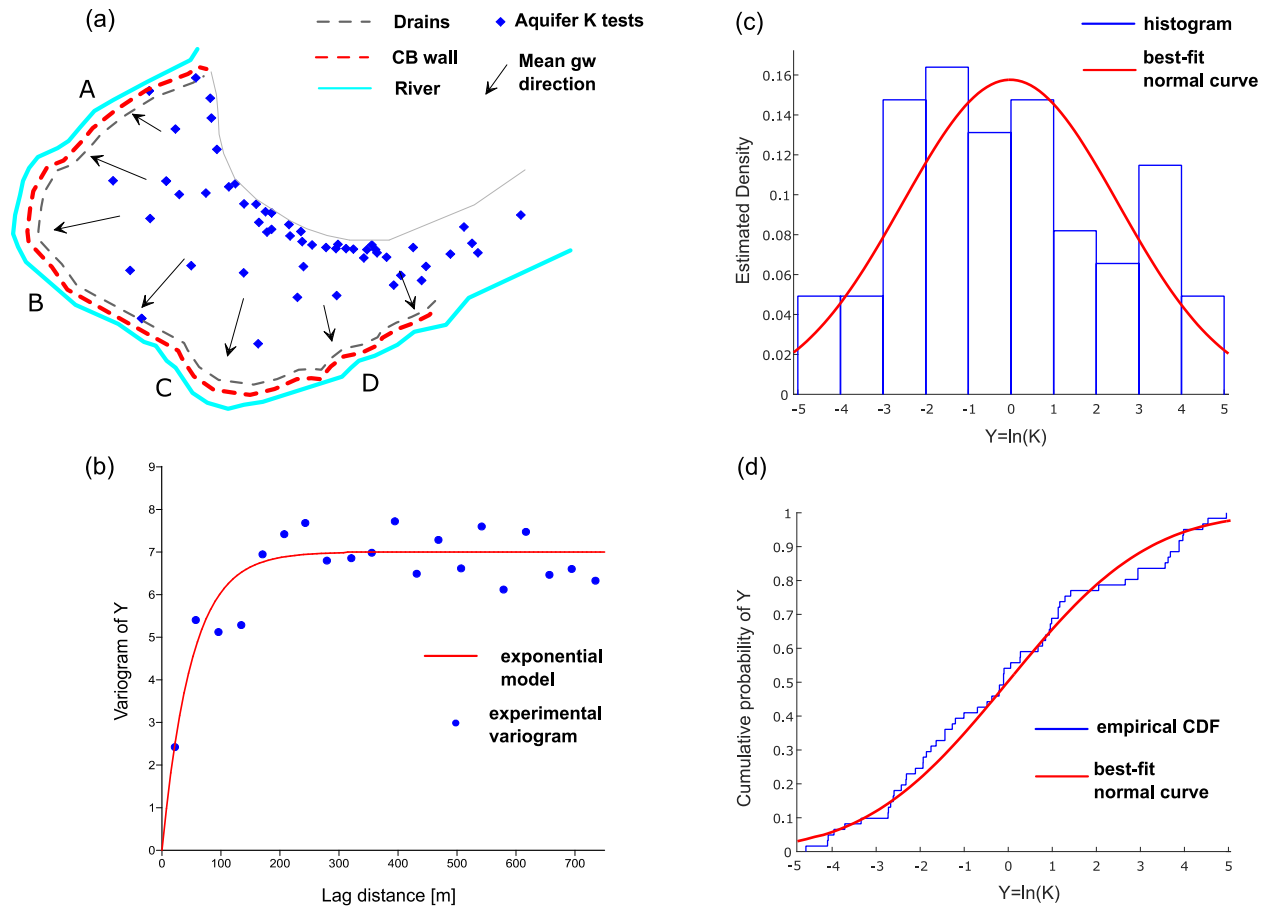
551



552

553 Figure 1 (a) Aerial view of the former chemical facilities. (b) Conceptual site model. JADV=inwards advective flux
554 (under pumped conditions), JDIFF= diffusive flux, Pz=piezometer; WT = water table. The dotted line indicates the
555 trace of the vertical section.

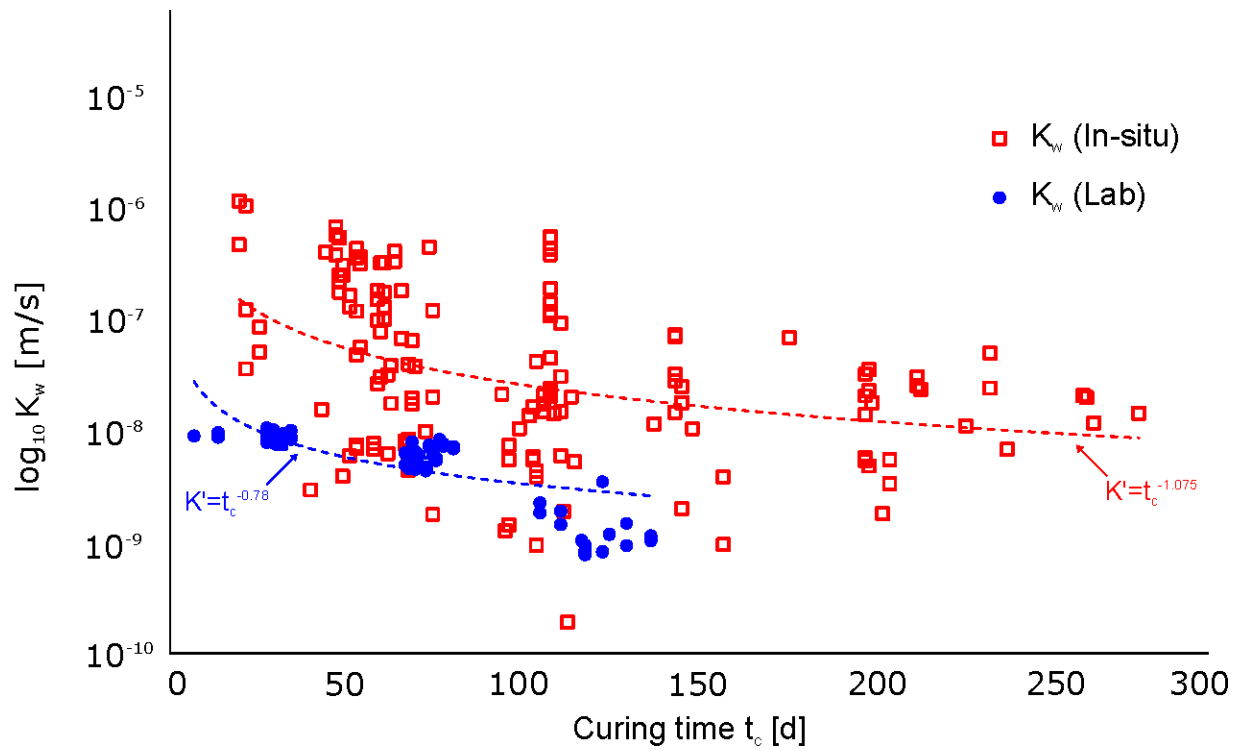
556



557

558 Figure 2 (a) Distribution of aquifer hydraulic testing locations (diamonds), the mean direction of the groundwater
 559 flow and geometry of the confinement area at the time the aquifer characterization. A,B,C,D are the zone labels for
 560 the CB walls hydraulic characterization. (b) Experimental and exponential variogram of Y_a . (c) Histogram and (d)
 561 cumulative empirical distributions of Y_a , respectively, along with the best-fit normal model.

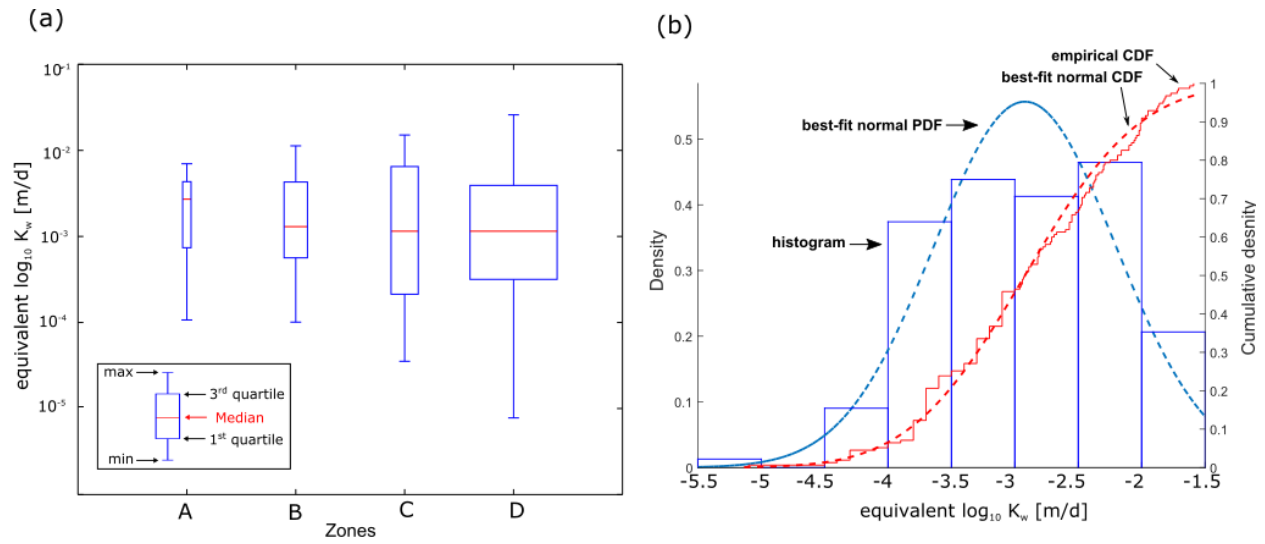
562



563

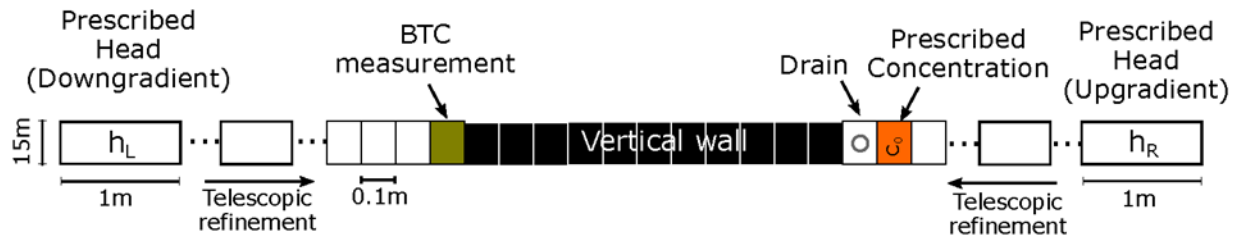
564 Figure 3 Evolution of measured K_w obtained from laboratory tests (blue) and from in-situ tests (red) at difference
 565 curing times (t_c). Here, $K' = K/K_0$, where K_0 is estimated from a best-fit regression curve of form $K = K_0 K_w^{-m}$ and
 566 m is the characteristic (scale-dependent) hardening factor.

567



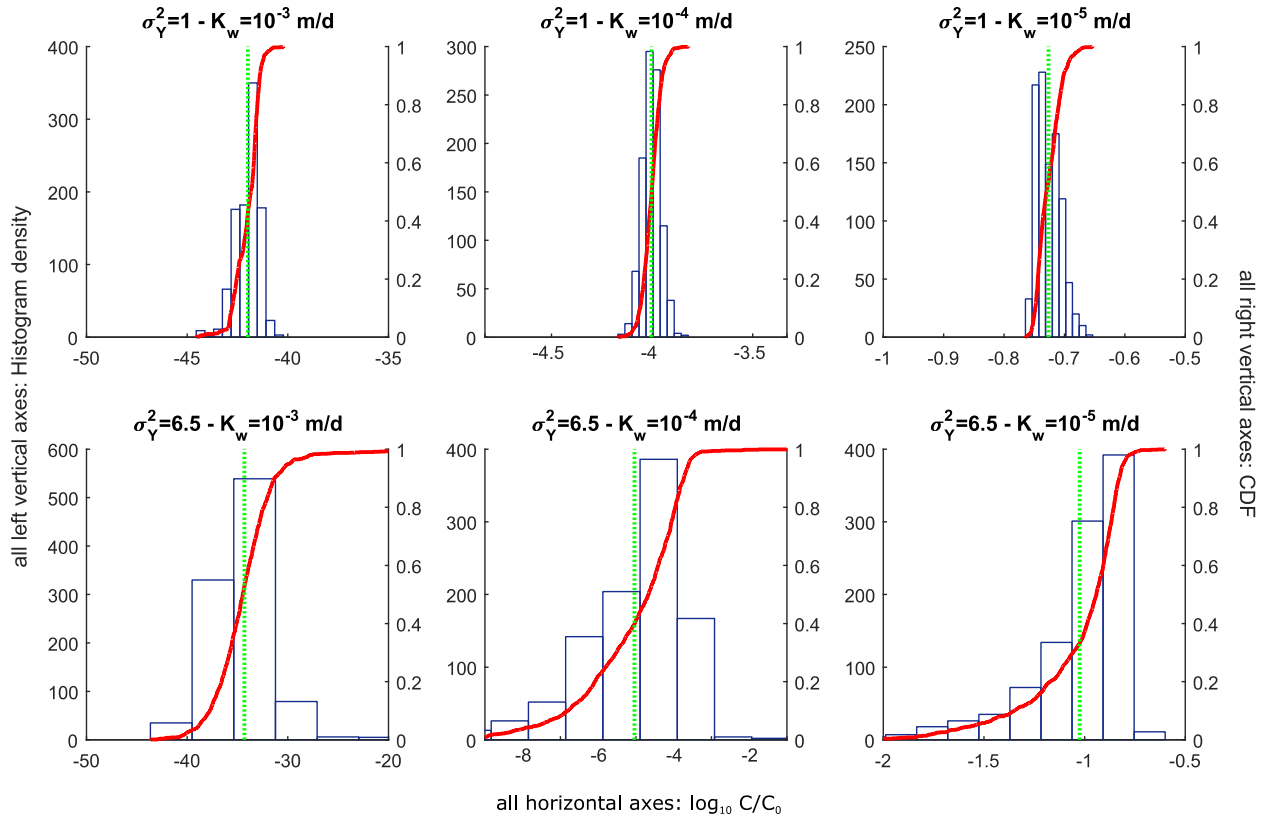
568

569 Figure 4 (a) Boxplots representing the statistical distribution of the equivalent $\log_{10} K_w$ estimated from in-situ tests
 570 and extrapolated at 280 days for the four different tested zones along the CB wall. The width of the boxes is
 571 proportional to the number of samples (n_s) used to calculate the empirical distributions. (b) Empirical histograms
 572 (blue) and cumulative density functions (red) of the equivalent $\log_{10} K_w$ at 280 days merging the four zones.
 573 Straight lines are the best-fit normal curves fitting the \log_{10} -transformed hydraulic conductivity values.



574

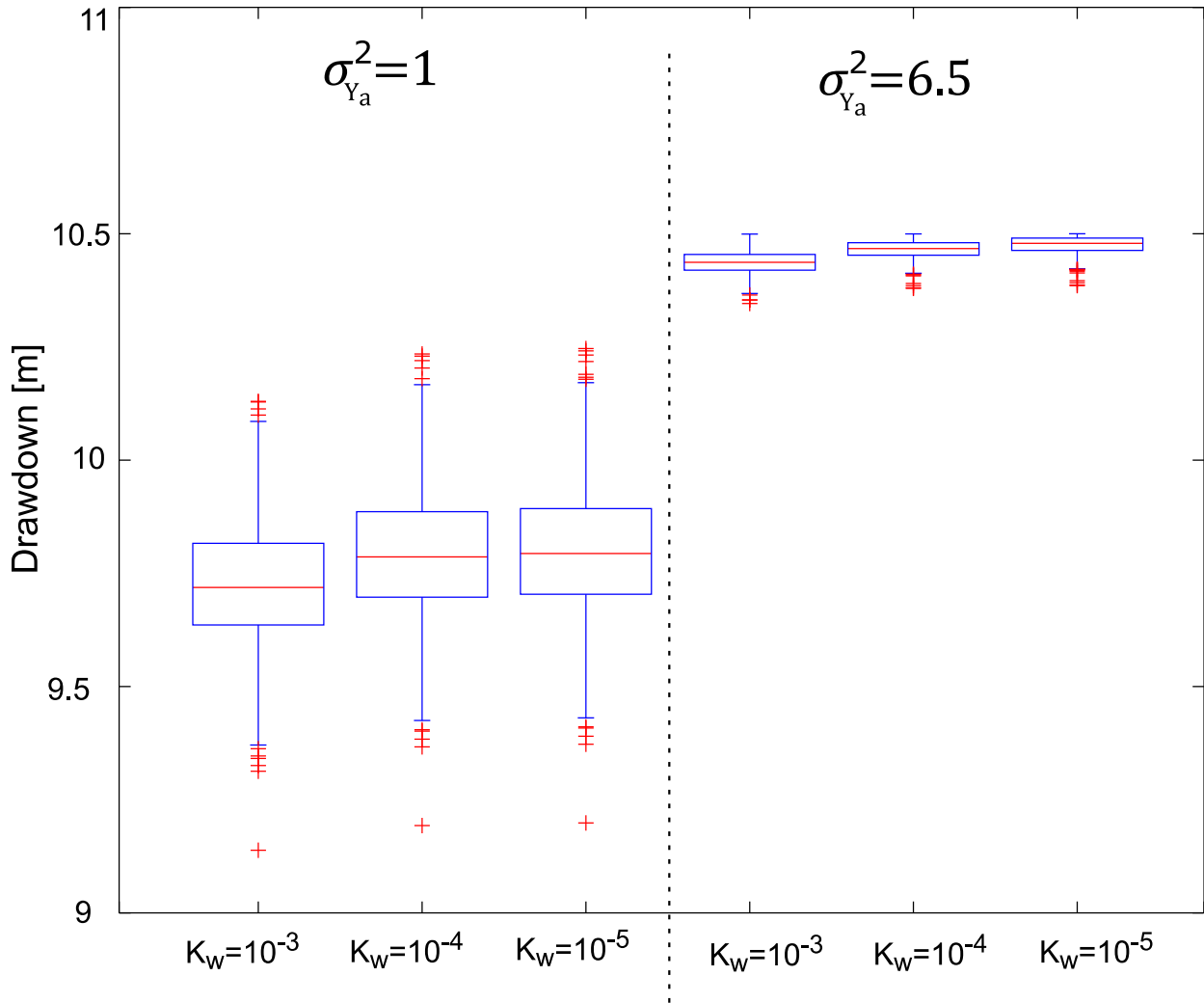
575 Figure 5 Conceptual model and numerical discretization of the domain for the stochastic solution of flow and
 576 transport in random domains. The size of the cells decrease telescopically from the sides towards the center of the
 577 domain. h_L and h_R are the downgradient and upgradient prescribed head boundary conditions, respectively. C_0 is the
 578 prescribed concentration at the continuous source nearby the drain, which has a steady discharge rate. The vertical
 579 walls are located between the drain and the cell where (resident) concentrations are measured in the form of
 580 breakthrough curve (BTC).



581

582 Figure 6 Summary of the stochastic analysis. Each panel shows the histogram of the distributions of resident
 583 concentrations monitored at the piezometer after 10 years from the initial spill from the ensemble of simulations,
 584 and the corresponding cumulative density function. The dotted green line is the ensemble average value, which
 585 suggests that the mean efficiency of the system and the variability around the mean are larger for the more
 586 heterogeneous set of simulations.

587



588

589 Figure 7 Boxplots representing the statistical distribution of maximum drawdown observed nearby the drain cell
 590 from the six analyzed scenarios. Note that greater drawdown is generated when the heterogeneity is higher (i.e. for
 591 higher variance of the log-transformed aquifer hydraulic conductivity, $\sigma_{Y_a}^2$). The units of the wall's hydraulic
 592 conductivity, K_w , are [m/d].

593

594 **References**

- 595 Baldi, F., Leonardi, V., D'Annibale, A., Piccolo, A., Zecchini, F., and Petruccioli, M. (2007). Integrated
596 approach of metal removal and bioprecipitation followed by fungal degradation of organic pollutants
597 from contaminated soils. *Eur. J. Soil Biol.* *43*, 380–387.
- 598 Bayer, P., and Finkel, M. (2006). Conventional and Combined Pump-and-Treat Systems Under
599 Nonuniform Background Flow. *Groundwater* *44*, 234–243.
- 600 Beretta, G.P. (2015). Some aspects of the state of the art of contaminated sites remediation in Italy.
601 *Acque Sotter. - Ital. J. Groundw.* 27–40.
- 602 Bouwer, H., and Rice, R.C. (1976). A Slug Test for Determining Hydraulic Conductivity of Unconfined
603 Aquifers With Completely or Partially Penetrating Wells. *Water Resour. Res.* *12*, 423–428.
- 604 Britton, J.P., Filz, G.M., Little, J.C., and Herring, W.E. (2002). Shape factors for single-well tests in soil-
605 bentonite cutoff walls. (Balkema, Rotterdam, Netherlands), pp. 639–644.
- 606 Britton, J.P., Filz, G.M., and Little, J.C. (2005). The Effect of Variability in Hydraulic Conductivity on
607 Contaminant Transport through Soil–Bentonite Cutoff Walls. *J. Geotech. Geoenvironmental Eng.*
- 608 Carreto, J.M.R., Caldeira, L.M.M.S., and Neves, E.J.L.M. das (2015). Hydromechanical Characterization of
609 Cement-Bentonite Slurries in the Context of Cutoff Wall Applications. *J. Mater. Civ. Eng.*
- 610 Choi, H., and Daniel, D.E. (2006). Slug Test Analysis in Vertical Cutoff Walls. I: Analysis Methods. *J.*
611 *Geotech. Geoenvironmental Eng.*
- 612 Choi, H.-J., Nguyen, T.-B., Lim, J., and Choi, H. (2014). Parametric study on cutoff performance of soil-
613 bentonite slurry wall: Consideration of construction defects and bentonite cake. *KSCE J. Civ. Eng.* *19*,
614 1681–1692.
- 615 Dagan, G. (1989). *Flow and transport in porous formations.* xvii + 465 pp.
- 616 Dai, Z., Ritzi Jr, R.W., Huang, C., Rubin, Y., and Dominic, D.F. (2004). Transport in heterogeneous
617 sediments with multimodal conductivity and hierarchical organization across scales. *J. Hydrol.* *294*, 68–
618 86.
- 619 Daniel, D.E. (1984). Predicting Hydraulic Conductivity of Clay Liners. *J. Geotech. Eng.*
- 620 D'Annibale, A., Ricci, M., Leonardi, V., Quaratino, D., Mincione, E., and Petruccioli, M. (2005).
621 Degradation of aromatic hydrocarbons by white-rot fungi in a historically contaminated soil. *Biotechnol.*
622 *Bioeng.* *90*, 723–731.
- 623 De Paoli, B., and Marcellino, P. (1992). Esperienze di isolamento mediante diaframmi, in: *Proc. of*
624 *the Course on Traitment and resting of polluted terrains (Trattamento e recupero dei terreni*
625 *contaminati)*, Dip. of Hydraulic. Environmental and Surveying Eng., Politecnico di Milano.

- 626 Devlin, J.F., and Parker, B.L. (1996). Optimum Hydraulic Conductivity to Limit Contaminant Flux Through
627 Cutoff Walls. *Groundwater* 34, 719–726.
- 628 Domenico, A. di, Felip, E.D., Ferri, F., Iacovella, N., Miniero, R., Tella, E.S. di, Tafani, P., and Baldassarri,
629 L.T. (1992). Determination of the composition of complex chemical mixtures in the soil of an industrial
630 site. *Microchem. J.* 46, 48–81.
- 631 Durante, G., and Grasso, F. (2010). L'ACNA di Cengio e la sua pesante storia ambientale (In Italian).
632 *Ecoscienza*.
- 633 Falasco, E., Bona, F., Ginepro, M., Hlubikova, ` , Hoffmann, L., and Ector, L. (2009). Morphological
634 abnormalities of diatom silica walls in relation to heavy metal contamination and artificial growth
635 conditions. *Water SA* 35.
- 636 Freeze, R.A. (1975). A stochastic-conceptual analysis of one-dimensional groundwater flow in
637 nonuniform homogeneous media. *Water Resour. Res.* 11, 725–741.
- 638 Gooverts, P. (1997). *Geostatistics for environmental applications* (Oxford University Press, USA).
- 639 Harbaugh, A.W., and McDonald, M.G. (1996). User's documentation for MODFLOW-96, an update to the
640 U.S. Geological Survey modular finite-difference ground-water flow model (U.S. Geological Survey ;
641 Branch of Information Services [distributor],).
- 642 Hudak, P.F. (2004). Augmenting Groundwater Monitoring Networks near Landfills with Slurry Cutoff
643 Walls. *Environ. Monit. Assess.* 90, 113–120.
- 644 Inyang, H.I., and Tomassoni, G. (1992). Indexing of long-term effectiveness of waste containment
645 systems for a regulatory impact analysis (A Technical guidance document, Office of solid Waste, U.S.
646 EPA, Washington, DC, pp29).
- 647 Jankovic, I., Fiori, A., and Dagan, G. (2006). Modeling flow and transport in highly heterogeneous three-
648 dimensional aquifers: Ergodicity, Gaussianity, and anomalous behavior - 1. Conceptual issues and
649 numerical simulations. *Water Resour Res* 42, W06D12.
- 650 Joshi, K., Kechavarzi, C., Sutherland, K., Ng, M.Y.A., Soga, K., and Tedd, P. (2009). Laboratory and In Situ
651 Tests for Long-Term Hydraulic Conductivity of a Cement-Bentonite Cutoff Wall. *J. Geotech.*
652 *Geoenvironmental Eng.*
- 653 Kaleris, V.K., and Ziogas, A.I. (2013). The effect of cutoff walls on saltwater intrusion and groundwater
654 extraction in coastal aquifers. *J. Hydrol.* 476, 370–383.
- 655 Kawas, M.L., and Karakas, A. (1996). On the stochastic theory of solute transport by unsteady and steady
656 groundwater flow in heterogeneous aquifers. *J. Hydrol.* 179, 321–351.
- 657 Khandelwal, A., Rabideau, A., and Su, J. (1997). One-dimensional contaminant transport model for the
658 design of soil-bentonite slurry walls (USDOE, Washington, DC (United States)).
- 659 Kitanidis, P.K. (1988). Prediction by the method of moments of transport in a heterogeneous formation.
660 *J. Hydrol.* 102, 453–473.

- 661 Lim, J., Lee, D., Zlotnik, V.A., and Choi, H. (2014). Analytical Interpretation of Slug Test in a Vertical Cutoff
662 Wall. *Groundwater* 52, 284–290.
- 663 Maione, U. (1995). Methods for Restoring Aquifers. In *Advanced Methods for Groundwater Pollution*
664 *Control*, G. Gambolati, and G. Verri, eds. (Springer Vienna), pp. 265–278.
- 665 Malusis, M.A., and McKeehan, M.D. (2013). Chemical Compatibility of Model Soil-Bentonite Backfill
666 Containing Multiswellable Bentonite. *J. Geotech. Geoenvironmental Eng.*
- 667 Manassero, M. (1994). Hydraulic conductivity assessment of slurry wall using piezocone test. *J Geotech*
668 *Geoenv Eng ASCE* 120, 1725–1746.
- 669 Matheron, G. (1967). *Elements Pour Une Theorie des Milieux Poreux* (Masson et Cie, Paris).
- 670 Molinari, A., Pedretti, D., and Fallico, C. (2015). Analysis of convergent flow tracer tests in a
671 heterogeneous sandy box with connected gravel channels. *Water Resour. Res.* 51, 5640–5657.
- 672 Neville, C.J., and Andrews, C.B. (2006). Containment Criterion for Contaminant Isolation by Cutoff Walls.
673 *Groundwater* 44, 682–686.
- 674 Nguyen, T.-B., Lee, C., Kim, S., and Choi, H. (2010). Modification of the Bouwer and Rice Method to a
675 Cutoff Wall with a Filter Cake. *Groundwater* 48, 898–902.
- 676 Pedretti, D., Masetti, M., Marangoni, T., and Beretta, G.P. (2011). Slurry wall containment performance:
677 monitoring and modeling of unsaturated and saturated flow. *Environ. Monit. Assess.* 184, 607–624.
- 678 Pedretti, D., Masetti, M., Beretta, G.P., and Vitiello, M. (2013a). A Revised Conceptual Model to
679 Reproduce the Distribution of Chlorinated Solvents in the Rho Aquifer (Italy). *Groundw. Monit.*
680 *Remediat.* 33, 69–77.
- 681 Pedretti, D., Fernández-García, D., Bolster, D., and Sanchez-Vila, X. (2013b). On the formation of
682 breakthrough curves tailing during convergent flow tracer tests in three-dimensional heterogeneous
683 aquifers. *Water Resour. Res.* 49, 4157–4173.
- 684 Pedretti, D., Fernández-García, D., Sanchez-Vila, X., Bolster, D., and Benson, D.A. (2014). Apparent
685 directional mass-transfer capacity coefficients in three-dimensional anisotropic heterogeneous aquifers
686 under radial convergent transport. *Water Resour. Res.* 50, 1205–1224.
- 687 Remy, N., Boucher, A., and Wu, J. (2009). *Applied Geostatistics with SGeMS. A User's Guide.*
- 688 Renard, P. (2007). Stochastic Hydrogeology: What Professionals Really Need? *Ground Water* 45, 531–
689 541.
- 690 Russell, K.T., and Rabideau, A.J. (2000). Decision Analysis for Pump-and-Treat Design. *Groundw. Monit.*
691 *Remediat.* 20, 159–168.
- 692 Sanchez-Vila, X., and Fernández-García, D. (2016). Debates—Stochastic subsurface hydrology from
693 theory to practice: Why stochastic modeling has not yet permeated into practitioners? *Water Resour.*
694 *Res.* 52, 9246–9258.

- 695 Sanchez-Vila, X., Carrera, J., and Girardi, J.P. (1996). Scale effects in transmissivity. *J. Hydrol.* 183, 1–22.
- 696 Tartakovsky, D.M. (2007). Probabilistic risk analysis in subsurface hydrology. *Geophys Res Lett* 34,
697 L05404, doi:10.1029/2007GL029245.
- 698 Torstensson, B.-A. (1984). A New System for Ground Water Monitoring. *Groundw. Monit. Amp*
699 *Remediat.* 4, 131–138.
- 700 Turchan, G.T., Richardson, I.K., and Norman, A.W. (1989). Groundwater cutoff walls: Application at
701 hazardous waste sites. Focus Conference on Eastern Regional Ground Water Issues, NWWA-WCGR.
- 702 Wu, Y.-X., Shen, S.-L., and Yuan, D.-J. (2016). Characteristics of dewatering induced drawdown curve
703 under blocking effect of retaining wall in aquifer. *J. Hydrol.* 539, 554–566.
- 704 Xanthakos, P.P. (1979). *Slurry walls* (McGraw-Hill, New York.).
- 705 Zheng, C., and Wang, P.P. (1999). MT3DMS, A Modular Three-Dimensional Multispecies Transport
706 Model for Simulation of Advection, Dispersion, and Chemical Reactions of Contaminants in Groundwater
707 Systems; Documentation and User’s Guide. University of Alabama, Tuscaloosa.
- 708